[Article Full Title]

Intermediate tissue oxygen level is required to observe murine FLASH skin sparing

[Short Running Title]

Oxygen impact on murine FLASH skin sparing

[Author Names]

David I. Hunter, M.S[1†*], Jacob P. Sunnerberg, Ph.D.[1,2*], Armin D. Tavakkoli, A.B.[1,3], Austin M. Sloop, M.S[1], Beverly Allen, B.S.[1], Jiang Gui, Ph.D.[4], Xu Cao, Ph.D.[1], Rongxiao Zhang, Ph.D.[5], Harold M. Swartz, M.D. Ph.D.[1,6], David J. Gladstone, Sc.D.[1,7], Lesley A. Jarvis, M.D Ph.D.[7], P. Jack Hoopes, D.V.M, Ph.D.[1,8], Brian W. Pogue, Ph.D.[1,9#]

[Author Institutions]

[1]Thayer School of Engineering at Dartmouth, Hanover NH 03755 USA
[2]Department of Radiation Oncology, Perelman School of Medicine, University of Pennsylvania, Philadelphia, PA
[3]Geisel School of Medicine at Dartmouth, Hanover NH 03755 USA
[4]Biomedical Data Science, School of Medicine at Dartmouth, Hanover NH 03755 USA
[5]Department of Radiation Oncology, University of Missouri, Columbia MO
[6]Department of Radiology, Geisel School of Medicine at Dartmouth, Hanover NH 03755 USA
[7]Department of Radiation Oncology & Applied Sciences, Geisel School of Medicine at Dartmouth, Hanover NH 03755 USA
[8]Department of Surgery, Geisel School of Medicine at Dartmouth, Hanover NH 03755 USA
[9]Department of Medical Physics, University of Wisconsin School of Medicine and Public Health, Madison WI 53705 USA

* Equal contribution

[Corresponding Author Name & Email Address]

[#] Corresponding author contact information: Brian.W.Pogue@dartmouth.edu

[Author Responsible for Statistical Analysis Name & Email Address]

[†]Author responsible for statistical analysis: David.I.Hunter.TH@dartmouth.edu

[Conflict of Interest Statement for All Authors]

Disclosures: B.W.P reports support for attending meetings and/or travel from DoseOptics, LLC, multiple patents planned, issued or pending on Cherenkov imaging held by Dartmouth College and DoseOptics, LLC, and stock or stock options from DoseOptics, LLC. H.M.S reports consulting fees for Xeno Therapeutics, and multiple patents on EPR held by Dartmouth College.

[Funding Statement]

The authors acknowledge funding for this work from the National Cancer Institute through contract U01 CA260446 and grant R01 CA271330, as well as shared resources of the Dartmouth Cancer Center P30 CA023108, and the UW Carbone Cancer Center P30 CA014520.

[Data Availability Statement for this Work]

Research data will be shared upon reasonable request to the corresponding author.

[Acknowledgements]

Oxyphor PdG4 was supplied through collaboration with Professor Sergei Vinogradov at the University of Pennsylvania.

Abstract

Purpose: This study evaluated the hypothesis that baseline tissue oxygen (pO_2) would modulate FLASH damage sparing in murine skin, comparing MeV ultra-high dose rate (UHDR) versus conventional dose rate (CDR).

Methods and Materials: Murine leg skin pO_2 was systematically varied and measured during irradiation from a Mobetron 9 MeV linac at 25 Gy, comparing UHDR (≈240 Gy/s) to CDR (≈0.16 Gy/s), for skin damage outcomes. Radiolytic oxygen consumption, g_{O2} (mmHg/Gy), was also quantified in vivo. Baseline tissue pO_2 was systematically modulated in 5 different treatment cohorts, using known methods of the inhaled gas (room air, 100% oxygen, or carbogen) and through applied limb vascular compression (partial or full). Induced skin damage was scored daily per mouse, and averaged in each group.

Results: FLASH skin sparing was observed in groups with partial leg clamping (pO_2≈7±4mmHg), inhaled air (pO_2≈12±6mmHg) and oxygen (tissue pO_2≈16±4mmHg), while reduction in time-to-damage was significant just in the air inhalation group. No FLASH effect was observed at zero oxygen, via complete blood flow occlusion (pO_2≈0±1mmHg), or when modulated by inhaled carbogen (pO_2≈21±7mmHg). In vivo measure of radiolytic consumption, g_{O2}, correlated to initial

pO2 when FLASH was present ($pO_2 \approx 4$-16mmHg) and saturated above $pO_2 > 16$mmHg. Inspired carbogen induced highest the pO_2 and maximum damage at 25 Gy. Reductions in dose to 20 and 15 Gy reduced skin damage, but did not result in FLASH sparing.

Conclusions: These findings indicate that tissue pO_2 directly modulates in vivo FLASH skin tissue sparing, requiring roughly room air or 100% oxygen anesthetic gas levels for this effect to be present. The FLASH effect is diminished by the absence of oxygen or from abnormally high oxygen values. Variations in dose does not appear to alter this observation at carbogen induced pO_2 levels, and the consumption rate of oxygen is directly correlated to the baseline value when the FLASH effect is present.

Introduction

Oxygen plays a fundamental role in radiation therapy as demonstrated in cell survival and in vivo studies where the absence of oxygen (hypoxia) can dramatically reduce radiation killing efficacy by a factor of ≈2.7, known as the oxygen enhancement ratio (OER) [1]. Oxygen is one of the most reactive molecules in biology, and its presence amplifies radiation effectiveness through complex reactive oxygen species (ROS) that react with nearly all biological molecules, including oxidation of DNA to extend and fixate it via peroxyl formation [2]. Recent studies have shown that oxygen acts as a modulator of the observed FLASH effect [3-7], a phenomenon characterized by reduced normal tissue toxicity under ultra-high dose rate (UHDR) radiation therapy while maintaining tumor control [8]. A key distinction between tumors and healthy tissues lies in their baseline oxygenation, with solid tumors typically being hypoxic (0-10 mmHg) as compared to normal tissues (10-40 mmHg) [9]. This difference may be particularly relevant given that oxygen is one of the most significant modifiers of radiation damage, thought to be primarily through the formation of peroxyl radicals that "fix" radiation-induced damage [10, 11]. Perhaps the most compelling aspect of this is that true pO_2 values are rarely known for any tissue being irradiated, and yet the OER effect can half or double the effective damage from any given dose delivery, and alter the tumor to normal tissue damage ratio. In this study, we examined how prospectively measuring and modulating the tissue pO_2 might affect the observation of the FLASH effect.

One of the more interesting features of UHDR delivery is that the dose and oxygen damage timelines are sufficiently faster than the oxygen supply from the capillaries, so that it is possible to directly measure the oxygen consumed *in vivo* from the radiation ROS [12-15]. A series of studies have shown how to quantify radiolytic oxygen consumption under UHDR conditions, and

in solutions the consumption per unit dose of radiation at UHDR is lower than that at CDR [12, 16-19]. This suggests that UHDR may induce less ROS than CDR at isodose levels and thereby potentially less damage. However, these observations have only been effective *in vitro* solutions and CDR measurements of this are not easily possible.

In vivo studies have shown stable and repeatable murine skin tissue oxygen consumption rates [13, 15, 20], and reach a plateau of ≈ 0.2 - 0.3 mmHg/Gy above 20 mmHg baseline tissue oxygenation [15]. This finding corroborates previous *in vitro* studies [17-19, 21, 22] showing that oxygen consumption g-value (g_{O2}) systematically decreases with oxygen tension below 20 mmHg, with a 50% reduction at approximately 8 mmHg, however no change is observed in g_{O2} at higher levels. Even more important than this is the observation that the apparent g_{O2} values are lower in tumor tissue than normal tissues[23], suggesting that there may be a reduction in ROS mediated damage. While these studies establish a clear relationship between tissue oxygenation and radiation-induced oxygen consumption, the correlation between these radiation-chemical patterns and differential tissue response under UHDR conditions remains unexplored.

Given the well-characterized relationship between tissue oxygenation levels and radiation damage, and the interesting capability to measure g_{O2} *in vivo* [15], this study was developed to explore the relationship between the FLASH effect, oxygen, dose and g_{O2} metrics in a radiation skin response study. Part of the outcome of this work was to determine if tissue pO_2 and/or g_{O2} are mechanistically linked to the FLASH-RT effect. Additionally, a secondary goal was to assess if pO_2 or g_{O2} measurements provide beneficial information for optimizing the FLASH effect and revealing necessary initial conditions in tissue. Given, the dominance of oxygen inducing reactive

oxygen species in radiotherapy that induce substantial damage, understanding how oxygen levels can affect the observation of the FLASH effect was motivation for this work.

Methods

Animals

This vertebrate animal study protocol was approved by the institutional IACUC committee, and all procedures carried out complied with this. One-hundred and fifty male Albino B6 mice were purchased (Jackson Laboratories, Cambridge, MA) at 8-10 weeks of age and housed in the institution vivarium. The population was divided into two groups, for either UHDR or conventional dose rate (CDR), with each group further split into five oxygenation cohorts. Each cohort consisted of 10-11 mice. There is a well-known sex differential in radiation response [1, 24], which has been documented in the FLASH effect and so for simplicity only male mice were studied here [7].

Fur on the left leg and surrounding area of each mouse was shaved 3 days prior to irradiation. One hour before irradiation, all mice underwent a 3-minute anesthesia induction with 3% isoflurane the oxygen probe Oxyphor PdG4 (Oxygen Enterprises, Philadelphia, PA), at 200µM in 0.05 mL in phosphate buffer solution was systemically administered into the retro-orbital space, with the oxygen measurement procedure described further below. The mice were then re-anesthetized for radiation delivery, using isoflurane at 3% for induction (delivered at 500 ml/min for 3 minutes) and maintained at 1.5% (delivered at 100 ml/min), under three different gas conditions: room air, 100% oxygen, or carbogen, and three different levels of vascular clamping: no clamping, partial clamping and complete clamping. The anesthesia/gas inhalation timing followed the protocol

reported by Tavakkoli et al.[7]. A heating pad was placed underneath each mouse to maintain consistent body temperature.

Radiation Delivery & Dosimetry

Irradiations were performed using a UHDR-capable Mobetron electron accelerator (IntraOp Inc., Sunnyvale, CA) designed for research use. The radiation field was shaped by a custom-designed collimator creating a 1.6 cm diameter circular treatment area, positioned on each mouse's left flank. To ensure accurate dosimetry and simultaneous oxygen measurements, the experimental setup incorporated a 3-D printed PETG cone with integrated holders for both an EDGE™ Detector (Sun Nuclear Corp, Melbourne, FL) and for oxygen measurement via a fiber-coupled phosphorimeter. This arrangement positioned the measurement devices upstream of the mouse while maintaining field alignment and preventing beam perturbation. To replicate conditions known to induce a FLASH sparing effect, all mice received a single-fraction dose to the left flank skin using a 1.6 cm circular field, under either CDR or UHDR delivery modes [25].

Dosimetric accuracy was ensured through calibration of the EDGE™ Detector against a flashDiamond detector (PTW, Freiburg, Germany), specifically designed for UHDR applications. The calibration was performed under identical geometric and delivery conditions as the animal irradiations, establishing a conversion factor between diode readings and delivered radiation fluence. Both detectors have been validated for UHDR dosimetry in previous studies by Rahman et al. and Tessonnier et al. [26, 27]. Temporal pulse information was measured and verified using the Beam Current Transformers (BCTs) installed in the head of the Mobetron, with dosimetry measurements included in Table 1.

Delivery Parameter	UHDR 25 Gy	UHDR 20 Gy	UHDR 15 Gy	CDR
SSD (cm)	37.0	37.0	37.0	46.0
Dose (Gy)	24.8 ± 0.4	20.4 ± 0.1	15.6 ± 0.2	24.9 ± 0.50 19.9 ± 0.03 14.9 ± 0.01
PRF (Hz)	90	90	90	30
D_M (Gy/s)	248 ± 4.0	230 ± 1.5	234 ± 2.9	0.16 ± 0.01
Pulse Width (μs)	3.2	3.2	3.7	1.2
No. of Pulses	10	8	6	
Dose/Pulse (Gy)	2.48 ± 0.04	2.55 ± 0.01	2.61 ± 0.03	
D_P (Gy/s)	$7.76 \times 10^5 \pm 0.12 \times 10^5$	$7.91 \times 10^5 \pm 0.05 \times 10^5$	$7.06 \times 10^5 \pm 0.09 \times 10^5$	

Table 1: *Beam delivery parameters for UHDR and CDR irradiations. Key characteristics include source-to-surface distance (SSD), pulse repetition frequency (PRF), pulse width, dose per pulse, instantaneous dose rate (D_P), mean dose rate (D_M), and total dose delivered, with values here reported as delivered with standard deviation values.*

Skin Damage Assay

Following radiation delivery, animals were monitored daily to visually score the progression of skin damage, via fixed geometry white light imaging. The primary endpoint of the study was the magnitude of skin damage score at the irradiation site, with a secondary measure of number of days to skin ulceration, consistent with previous UHDR studies investigating skin response [28-30]. The skin damage scoring scale was similar to that previously published by Noda et al. [31], shown in Table 2. As stated previously, the primary survival endpoint of this study was skin ulceration across the irradiation area, which corresponds to a skin score of 2 on this guide. This score was chosen because the observation of distinct ulceration onset was determined to be the most objectively binary decision point between graders for onset of damage. Additionally, each mouse was survived and monitored daily until a skin score of 3 was reached, at which point the mouse was sacrificed based upon IACUC guidance. At the conclusion of the study, 51 days post-

irradiation, all remaining mice were sacrificed regardless of skin score. Daily reading scores for each mouse were determined with knowledge and consideration of previous daily scores to track damage progression over time, while the mouse groups (UHDR, CDR, oxygen conditions) were blinded from the grader.

Mouse Skin Reaction Scoring Scale	
Score	Description
0	Normal appearance; no visible changes
0.5	Questionable change; difficult to distinguish from normal
0.75	Mild abnormality; subtle changes visible
1	Clear abnormality with erythema (reddening)
1.25	Pronounced erythema with white flaky skin and/or edema
1.5	Localized moist desquamation in a very small area with scaly or crusty appearance
1.75	Multiple small areas of moist desquamation
2	Extensive area breakdown with moist regions (ulceration)
2.5	Large confluent areas of moist desquamation with exudate
3	Severe skin breakdown affecting majority of irradiated area with extensive moist exudate

Table 2: *Radiation-induced skin damage numerical score scale used on daily photographs.*

Tissue Oxygenation Modulation

As detailed in Figure 1A, five oxygenation conditions were used to modulate tissue oxygen levels:

(i) inhaled room air with isoflurane anesthesia, with complete vascular compression to the leg above the irradiation site stopping all blood flow, ("Anoxic")

(ii) inhaled room air with isoflurane anesthesia, with partial vascular compression above the irradiation site inducing restricted blood flow, ("Hypoxic to mildly hypoxic)"

(iii) room air with isoflurane anesthesia, with no leg ligation (21% O_2), ("Mildly hypoxic")

(iv) inhaled 100% oxygen gas with isoflurane anesthesia, with no leg ligation, ("Normoxic to Mildly hyperoxic)

(v) inhaled carbogen gas, here defined as 95% O_2 with 5% CO_2, with anesthesia, with no leg ligation. ("Hyperoxic")

These approaches achieved a range of initial pO_2 levels from 0 to 43 mmHg in the skin of the mouse leg (Figure 1C). Both the UHDR (n = 54) and CDR (n = 55) groups were divided (n = 10-11) into these five cohorts to evaluate the FLASH effect under varying oxygen conditions, given the expected impact of oxygen levels on radiation response [1]. An additional cohort of UHDR (n = 20) and CDR (n = 21) mice were irradiated at 20 or 15 Gy dose levels under carbogen conditions due to assay saturation.

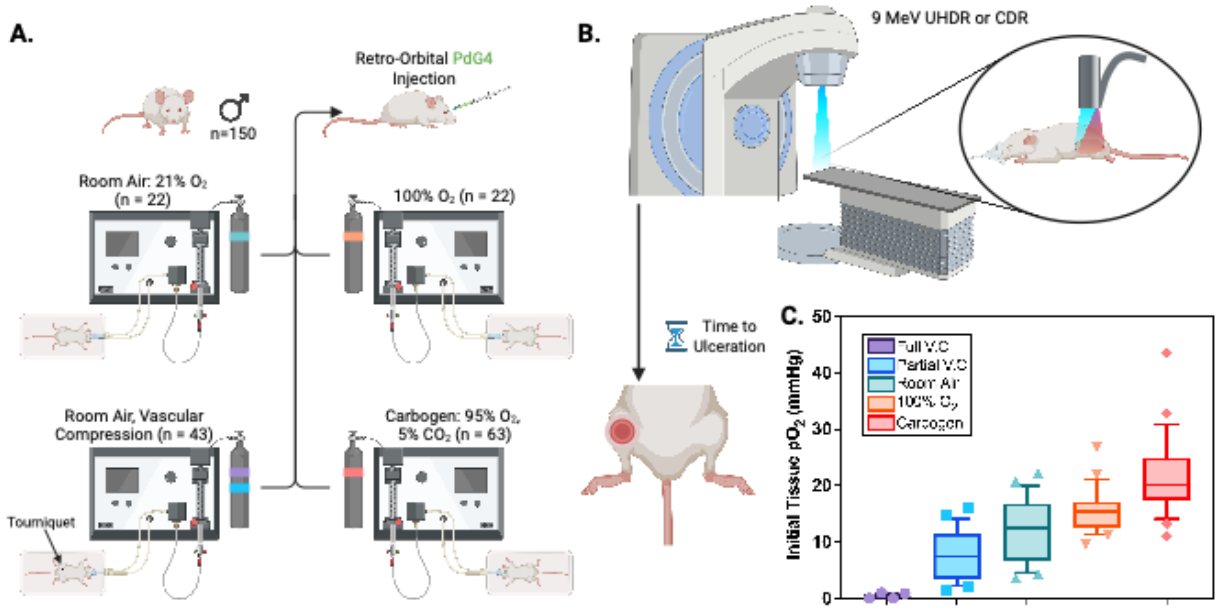

Figure 1: *A) Study design, including population distribution, probe injection method, and oxygenation cohorts (room air, room air with vascular compression, 100% oxygen, and carbogen). Gas canisters are color-coded to match the*

legend and data in (C). B) Schematic of radiation delivery setup, showing mouse positioning photograph, target dose, and primary endpoint. C) Box plots of initial tissue pO_2 at irradiation for each oxygen condition. Full vascular compression (V.C) with room air (purple), partial vascular compression with room air (blue), inhaled room air (green), inhaled 100% oxygen (orange), and inhaled carbogen (red).

In Vivo Oximetry Measurements

Real-time tissue oxygenation monitoring was accomplished using the phosphorescence-based oxygen probe Oxyphor PdG4 (Oxygen Enterprises, Philadelphia, PA). This dendritic probe operates via oxygen-dependent phosphorescence quenching and has undergone extensive validation for both *in vitro* and *in vivo* applications [32]. The Oxyphor PdG4 was administered through retro-orbital injection at 0.05 mL from 200 µM stock concentration, dissolved in phosphate buffer solution, approximately 60 minutes before radiation exposure to ensure adequate probe dispersion throughout the animal.

Oxygen measurements were captured using an OxyLED phosphorimeter system (Oxygen Enterprises, Philadelphia, PA). The system operated at a temporal resolution of 5 Hz (200 ms intervals), providing high-resolution oxygen dynamics during radiation delivery. To maintain measurement integrity while preventing radiation field interference, optical fibers were positioned at a 15 mm offset from the radiation field's center, with the main instrumentation and data acquisition computer situated approximately 1 meter from the radiation source. Conversion of phosphorescence lifetime measurements to absolute pO_2 values was performed using pre-measured calibration constants for this batch of Oxyphor [32].

This measurement approach enabled quantification of radiation-induced oxygen dynamics in real time. Baseline tissue oxygenation was established by averaging pre-irradiation measurements,

which were then subtracted from values obtained during and after radiation exposure [15]. The resulting differential oxygen measurements (ΔpO_2) were normalized to radiation dose, yielding oxygen consumption g-values (g_{O2}), expressed as mmHg per unit dose delivered (mmHg/Gy).

Statistical Analysis

For the radiation-induced skin damage scoring, numerical values were evaluated daily with the standardized scoring system (Table 2) by trained observers. To address the issue of mice being removed from the study upon reaching endpoints, a last-observation-carried-forward (LOCF) approach was used, where the final observed skin score for each mouse was carried forward for all subsequent time points. This method preserved the impact of severe reactions in statistical analysis and prevented skewing of data as mice were removed from study. Using this dataset, a mixed-effects analysis was used to compare UHDR and CDR cohorts within each oxygen environment over the post-irradiation observation period. The tests included dose rate and time as fixed effects, with individual mice as random effects to account for correlation among repeated measures within each mouse. This approach appropriately handled the ordinal nature of the skin score data while accommodating the longitudinal study design. Separate tests were run for each oxygenation conditions to determine whether dose rate significantly influenced skin damage progression under specific oxygen environments. The null hypothesis tested was that dose rate did not affect the progression of radiation-induced skin damage under equivalent oxygenation conditions. Statistical significance was defined as p-value ≤ 0.05.

To evaluate the difference in time to reach skin ulceration (score = 2 in Table 2), Kaplan-Meier survival analysis was used, displaying the proportion of mice that remained ulceration-free over the observation period. Separate curves were generated for UHDR and CDR treatment groups

within each oxygenation condition. Statistical comparisons between dose rate groups were performed using Log-Rank (Mantel-Cox) tests, with p-value ≤ 0.05 being considered statistically significant. This analysis allowed quantitative assessment of whether dose rate affects the timing and incidence of ulceration under controlled oxygen environments.

Comparison of oxygen consumption g-values and initial pO_2 values between mice that developed ulceration and those that remained ulceration-free was performed using Mann-Whitney U tests. The two experimental hypotheses (H_1) tested were that pO_2 and g_{O2} are lower for UHDR-irradiated mice that did not develop ulcers through the duration of the study. Statistical significance was defined as p-value ≤ 0.05.

Results

Skin pO_2 Observations in treatment groups

Tissue pO_2 values were varied through systematic induction of beathing gas or through clamping of blood flow, as illustrated in Figure 1. The induced ranges of skin pO_2, with mean and standard deviations illustrated in the graph in Figure 1C, were: (i) full vascular compression breathing room air, $pO_2 = 0.44 \pm 0.26$ mmHg, (ii) partial vascular compression breathing room air, $pO_2 = 7.4 \pm 4.3$ mmHg, (iii) freely breathing room air, $pO_2 = 11.9 \pm 5.6$ mmHg, (iv) freely breathing 100% oxygen, $pO_2 = 15.7 \pm 3.8$ mmHg, and (v) freely breathing carbogen, $pO_2 = 21.4 \pm 6.9$ mmHg. The total ranges were: full vascular compression 0-1.00 mmHg, partial vascular compression 1.4-16.0 mmHg, room air 3.6-22.3 mmHg, 100% oxygen 9.5-26.7 mmHg, and carbogen 11.1-43.4 mmHg. These breathing and clamping groups were taken as treatment cohorts for the remaining skin damage response studies in order to systematically study the variation in skin damage.

Skin Damage Outcome Difference

Radiation-induced skin damage was monitored daily for 51 days post-irradiation, and mean skin scores over time for each cohort are shown in Figure 2 for each of the five oxygen conditions (panels A-E), with both CDR and UHDR groups on each of these. To analyze these data, a mixed-effects analysis with LOCF was used to reveal any significant differences between UHDR and CDR treatment groups under specific oxygenation conditions. Mice in the room air cohort (Figure 2C) exhibited significantly reduced skin damage following UHDR treatment compared to CDR (p-value = 0.001). A similar FLASH sparing effect was observed in the room air with partial vascular compression (Figure 2B) cohort (p-value = 0.005), and to a lesser extent in the 100% oxygen (Figure 2D) cohort (p-value = 0.03), where UHDR-treated mice had less severe reactions throughout the study.

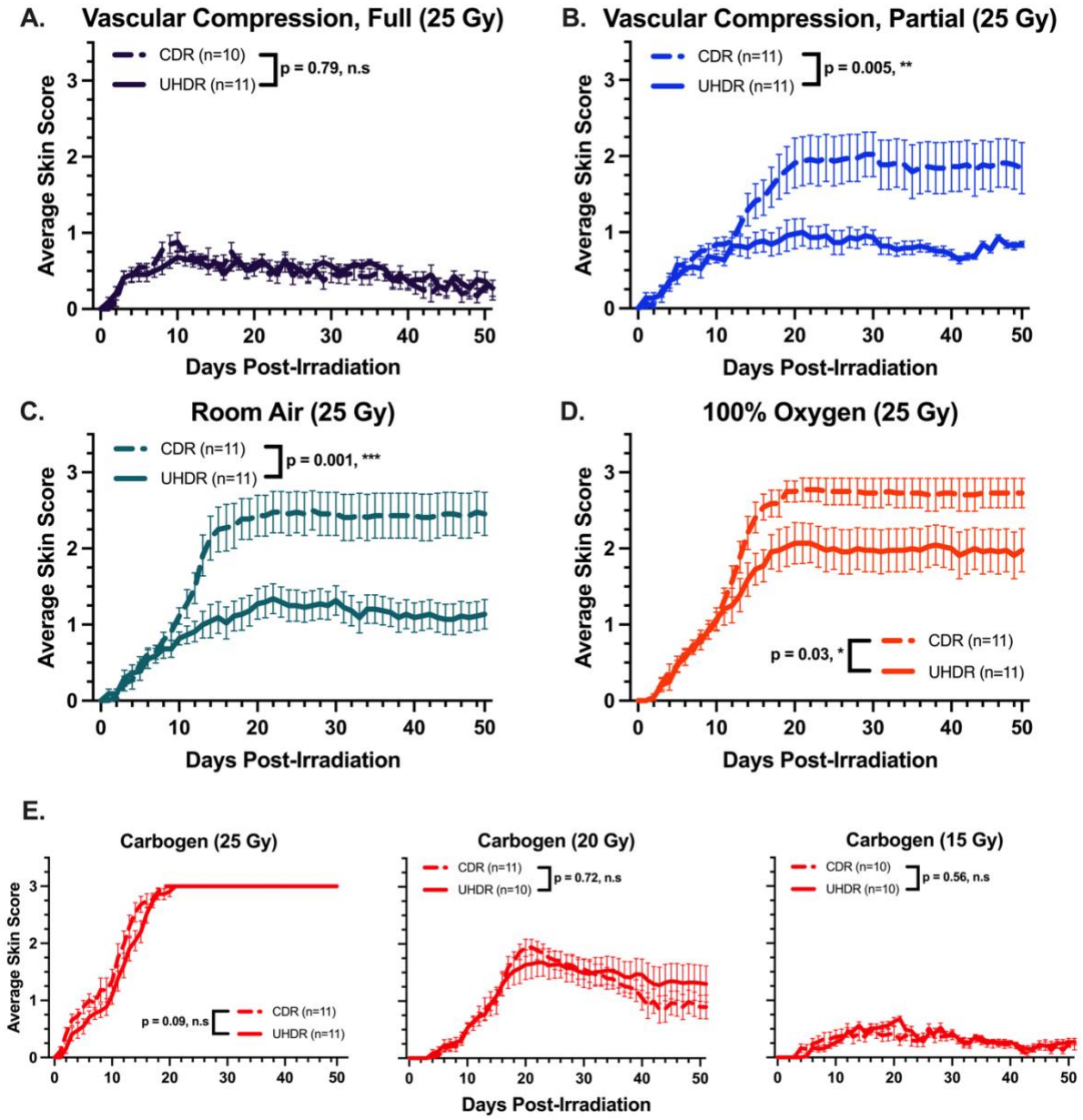

Figure 2: *Average skin lesion progression daily for each oxygenation cohort. Solid lines represent UHDR data, and dashed lines represent CDR data. Error bars show standard error of the mean. Statistical significance of dose rate effect is indicated as ***(p-value ≤ 0.001), **(p-value ≤ 0.01), *(p-value ≤ 0.05), and n.s. (p-value > 0.05). A) Room air with complete vascular compression (purple, p-value = 0.79). B) Room air with partial vascular compression (blue, p-value = 0.005). C) Room air (green, p-value = 0.001). D) 100% oxygen (orange, p-value = 0.03). E) Carbogen inhalation for each of 25 (left), 20 (middle) and 15 (right) Gy dose cohorts (red, p-values = 0.09, 0.72, 0.56).*

In contrast, no significant differences were observed between UHDR and CDR groups in the carbogen breathing cohorts. Mice in the 25 Gy carbogen (p-value = 0.09) group developed comparable skin damage, though not a significant sparing effect, although the skin damage scores saturated perhaps making it impossible to determine if there was skin damage lessening or not. As a result, additional mouse cohorts were treated with carbogen but using dose levels of 20 and 15 Gy (Figure 2E, middle and right), to reduce the overall damage and yield lower skin damage scores. These did not show a significant FLASH skin sparing effect (p-values = 0.72 & 0.56) despite not reaching assay saturation.

Skin ulceration endpoint & time to ulceration

The relationship between initial tissue oxygen tension (pO_2), oxygen consumption (g_{O2}), and ulceration is shown in Figure 3, with the raw data plotted in Figure 3 A, separating those animals that showed ulceration (red points) with those that did not (blue points). Among UHDR-irradiated mice, those that developed ulceration had significantly higher g_{O2}-values (0.17 ± 0.06 vs. 0.03 ± 0.07 mmHg/Gy, $p << 0.001$) and initial pO_2 levels (16.9 ± 5 vs. 3.8 ± 5.4 mmHg, p-value << 0.001) as compared to mice that remained skin ulcer-free, as shown in Figures 3 B and C. A linear regression fit of g_{O2} and pO_2 yielded an R^2 value of 0.84.

Kaplan-Meier survival curves are shown in Figure 4, illustrating the differences in time to ulceration between UHDR and CDR groups across oxygenation conditions. In the normoxic (room air) cohort, UHDR significantly delayed ulceration compared to CDR (p-value = 0.01), with 8 out of 11 UHDR-treated mice remaining ulcer-free for the full study duration. In contrast, the median time to ulceration for CDR-treated mice was 15 days.

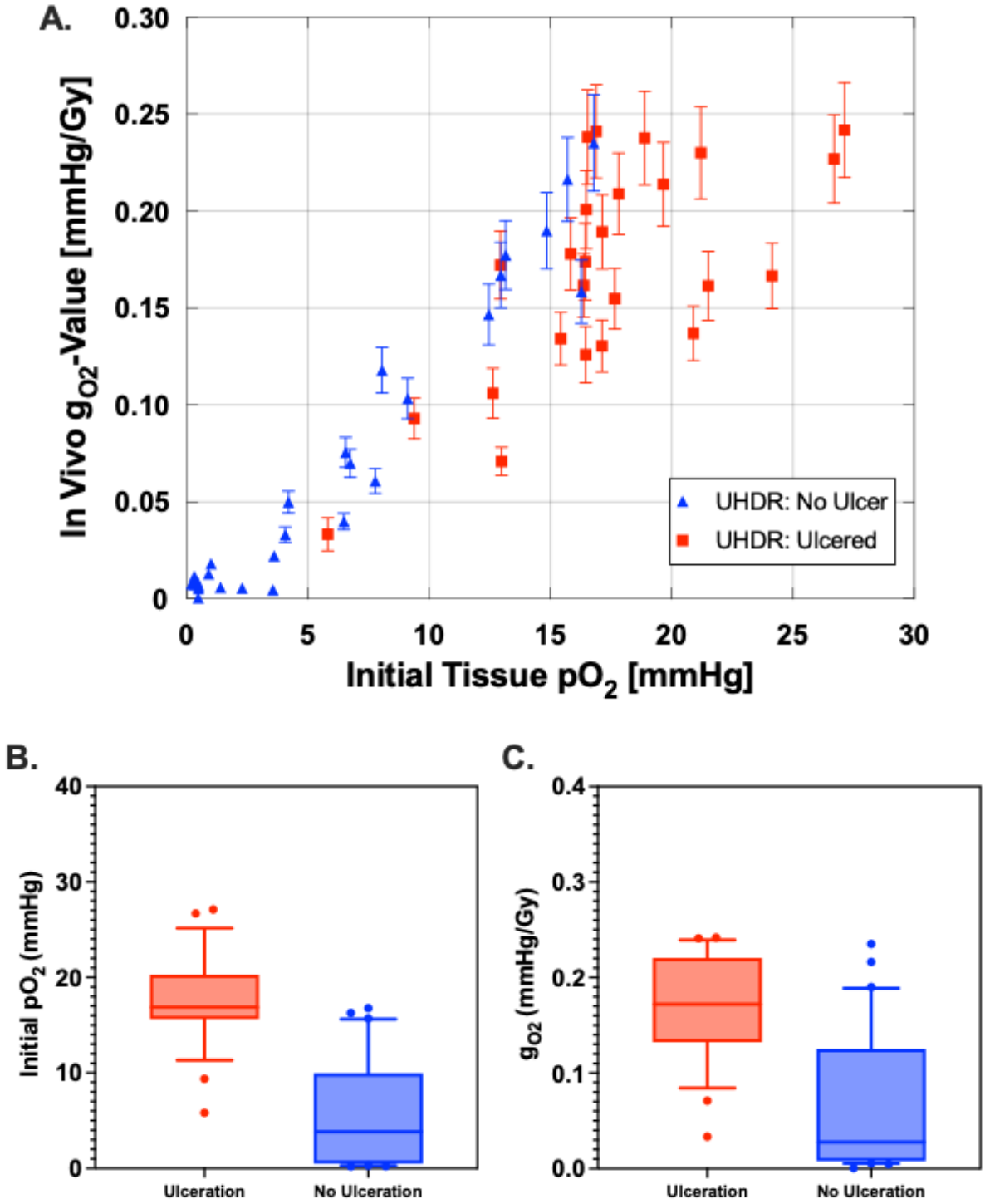

Figure 3: ***A)*** *In vivo g_{O2} measurements for UHDR-irradiated mice plotted against initial tissue pO_2. Each data point represents an individual mouse, with ulcered mice shown as red squares and non-ulcered mice as blue triangles. B)*

Box and whisker plots for initial pO_2 measurements between ulcerating (red) and non-ulcerating (blue) mice. C) Box and whisker plots for gO_2 measurements between ulcerating (red) and non-ulcerating (blue) mice.

Despite a significant difference in skin scores (Figure 2B, p-value = 0.005), the partial vascular compression cohort did not show a statistically significant FLASH effect for ulceration-free survival (Figure 4B, p-value = 0.16). This likely reflects an overall reduction in radiation-induced damage for CDR-treated mice in this cohort, leading to fewer ulceration events and in turn an underpowered log-rank test.

As opposed to the skin score analysis, no significant difference in ulceration-free survival was observed between UHDR and CDR groups in the 100% oxygen (Figure 4D, p-value = 0.15) cohort, and no difference was observed with the 25 Gy carbogen (Figure 4E, left, p-value = 0.46) cohort. These findings reinforce the oxygen dependence of the FLASH effect.

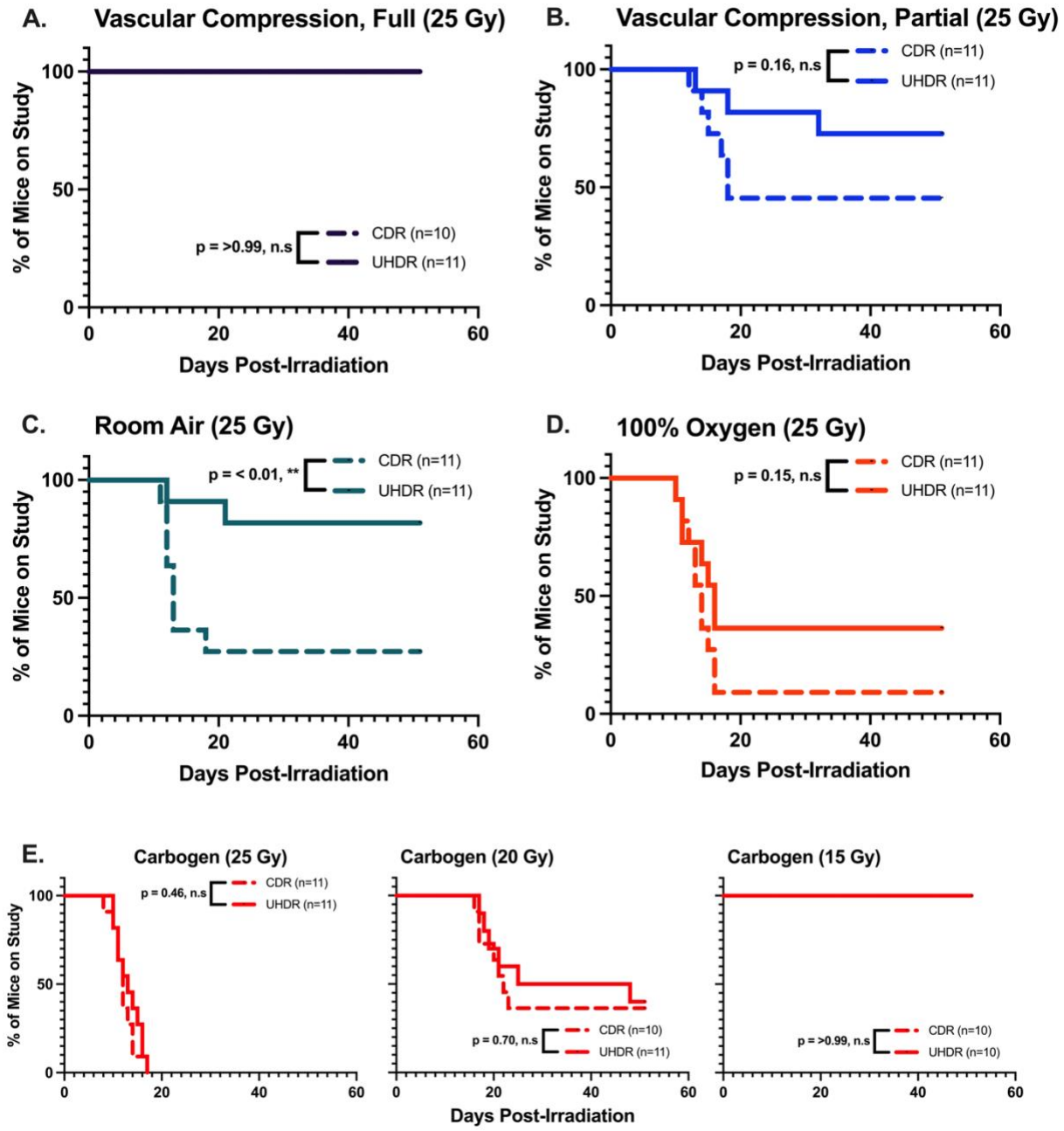

Figure 4: *Kaplan-Meier survival curves for ulcer-free survival of mice in each oxygenation cohort. Solid lines represent UHDR data, and dashed lines represent CDR data. Statistical significance of dose rate effect is indicated as ** (p-value ≤ 0.01), * (p-value ≤ 0.05), and n.s. (p-value > 0.05). A) room air with full vascular compression (purple, p-value = >0.99). B) Room air with partial vascular compression (blue, p-value = 0.16). C) Room air (green,*

p-value = < 0.01). D) 100% oxygen (orange, p-value = 0.15). E) Carbogen groups given 25 (left), 20 (middle) and 15 (right) Gy, respectively (red, p-value = 0.46, 0.70, >0.99).

Discussion

The FLASH effect of reducing damage with higher dose rate is now well established, but still the role of oxygen in terms of modulation and mechanism is unclear. In vitro data has been used to show that the FLASH damage reduction is present at mid-range oxygen values, disappearing at low oxygen and at high oxygen [33]. In vivo data has shown that UHDR radiation still effectively kills hypoxic tumors equivalent to CDR radiation [34], but it is not clear what happens when normal tissue is highly oxygenated or deoxygenated. Studies in rat brain showed the loss of the FLASH protective effect in the brain when supplemental oxygen was supplied to the anesthesia gas[35].

The present study was designed to test this phenomenon in a well-controlled in vivo model where oxygen could be systematically varied across the relevant range. The study results demonstrate that the observable difference in damage score exists between CDR and UHDR in this *in vivo* skin model, and we term this difference as FLASH skin sparing. The sparing is clearly dependent on initial tissue oxygen tension at the 25 Gy dose level investigated, being present in the ranges of oxygen found in the three conditions of room air, 100% oxygen and partial vascular compression ($pO_2 \approx$ 4-18 mmHg). However, when oxygen levels were modulated – either by complete anoxia (complete leg compression with ligation) inducing hypoxia ($pO_2 \approx 0$ mmHg) or hyperoxia, via carbogen inhalation (pO2 ≈ 15-28 mmHg), then the observation of FLASH tissue sparing was lost. Take together, these finding suggest that baseline oxygenation level is likely a critical factor influencing not just the observation of the FLASH effect but also is likely at least part of the mechanism causing the FLASH effect.

Examining the results from the hyperoxia carbogen group, it was noted that the *in vivo* assay saturated at the highest damage level for 25 Gy, with all mice reaching the maximum skin score of 3.0 in both UHDR and CDR groups. The skin damage scoring scale has a maximum of 3.0, potentially masking differences between treatment groups under hyperoxic conditions, rendering the assay to be non-useful for these high damage levels. Thus, the lower dose groups of 20 and 15 Gy were included in the study with carbogen to determine if lower damage levels would allow observation of FLASH tissue sparing at hyperoxia pO_2 levels. However as seen in Figures 2 and 4, there was no significant FLASH sparing observable when these lower dose levels were used. It is possible that finer measures of damage reduction may observe some difference here, but the magnitude of sparing does not seem to match that seen under partial vascular compression, room air and 100% oxygen breathing conditions. Thus, this data is consistent with a hypothesis that excess oxygen negates the FLASH effect, suggesting that perhaps the FLASH effect itself is dependent upon some spatial or temporal limitation in oxygen at the irradiation site.

At high oxygen levels, there is clearly higher damage, and the skin damage assay saturates, making this data uninterpretable as to whether there is a difference between UHDR and CDR groups (Figures 2E and 4E). Further analysis at lower dose levels (Figures 2F & 2G) additionally revealed that, still under elevated oxygen conditions, the FLASH effect is not observable in this assay and dose level. This result indicates that there may be an upper limit in oxygen availability beyond which even UHDR cannot prevent damage, consistent with previous studies [6, 7, 12, 14, 16, 18, 36, 37].

The link between oxygen tension and tissue damage is central to trying to understand the mechanisms of FLASH sparing, in terms of the underlying radiation chemistry. Under UHDR

conditions, the relationship between pO_2 and tissue toxicity appears to be altered such that the expected severity of damage following 25 Gy is reduced for all but anoxic and hyperoxic tissues, showing the FLASH effect is present. In the UHDR setting, oxygen is consumed rapidly in formation of peroxyl radicals, thereby causing fixation of the radiation induced damage in proteins and DNA. It has been previously shown in vitro that UHDR irradiation reduces oxygen consumption as compared to CDR, thereby supporting the hypothesis that UHDR leads to less peroxyl damage to DNA. However, linking in vitro data and DNA data to in vivo observations of damage is inherently challenging and at best a correlative link can be established, rather than causative links. Still the data here is consistent with the idea that oxygen is the mechanistic link leading to FLASH tissue sparing. Many studies have postulated and modeled transient oxygen depletion as a hypothesized mechanism for lower damage[38], although direct in vivo measurements of the level of consumption, here and in previous work [17, 20, 23], indicate that the level of oxygen consumed would not likely be sufficient for complete 'depletion' of local oxygen. Thus, there is not a clear explanation for this discrepancy and further data may be needed to determine if there are micro-localized depletions of oxygen or oxygen-related effects that are causative of reduced ROS damage in vivo.

Figure 2A relative to the other panels, provides important insight into the role and potential mechanism of FLASH occurrence, based upon the loss of any sparing under anoxic conditions. In this completely hypoxic cohort, overall skin damage was reduced compared to room air, and there was no difference in damage between UHDR and CDR groups. This observation could suggest that whatever is causing the FLASH tissue sparing must rely upon oxygen being present in the tissue.

The observations presented in Figure 3 provide a robust link between the radiation-induced oxygen consumption observed at UHDR and the biological FLASH effect. The relationship between radiation dose, dose rate, and tissue pO_2 suggests that the oxygen consumption g-value may serve as an important predictor for the onset of the FLASH effect. In fact, these findings build directly upon the concepts outlined in other publications in the broader FLASH field, which posit that oxygen chemistry under UHDR conditions is a determining factor for normal tissue sparing [13, 15-18]. The data presented herein support the idea that proper initial oxygenation levels are required to harness the full benefits of FLASH radiotherapy.

Overall, these results suggest that there is a need to carefully control and report tissue oxygenation conditions when designing preclinical FLASH studies, and this can be as subtle as causing variations in tissue oxygen from breathing gas, animal temperature or mouse positioning (i.e. leg clamping). The evidence that FLASH-sparing is contingent on tissue oxygen tension not only provides insight into the chemical mechanisms of radiation damage but also has significant implications for the clinical translation of FLASH radiotherapy. By clearly establishing the necessary initial conditions for FLASH sparing, our work contributes to a more mechanistic understanding of how dose rate and oxygen interact to modulate tissue responses. Future studies might extend these observations to other tissue types and dose rate regimes, further exploring how oxygen consumption and radical chemistry at UHDR influence both acute and long-term normal tissue outcomes. Additionally, experiments should be conducted which investigate the role of modulating oxygen in the FLASH effect tumor response under UHDR, although current data suggests that hypoxic tumors are effectively treated as well with UHDR as they are with CDR [34]. It is not clear if this effect is purely due to oxygen radiation chemistry change, or a mixture of this with things like differences in endothelial cell damage, because of oxygen or simply blood

flow. Further it is possible that there could be hypoxia inducible factor signaling changes or immune cell treatment effects that alter the magnitude of FLASH sparing and oxygen variation is simply a biomarker of this. Understanding how UHDR effectively influences the OER across varied tissues will be critical for refining the mechanistic basis of the FLASH effect and for optimally translating these findings into clinical practice.

Conclusion

This study demonstrated that in murine skin, tissue oxygen tensions achieved under room air anesthetic conditions are required for the most apparent observation of a skin FLASH sparing effect from UHDR versus CDR irradiation. Under partial vascular compression (hypoxic to mildly hypoxic), room air (mildly hypoxic) and 100% oxygen (normoxic to mildly hyperoxic) conditions, UHDR treatment resulted in a significant reduction in overall tissue damage compared to conventional dose rate exposures, and only the partial vascular compression condition achieved a significant reduction in overall ulceration. Hyperoxic skin with elevated local oxygen tension from carbogen breathing animals achieved maximal damage, and did not demonstrate any UHDR induced FLASH sparing, at any dose level studied. Anoxic skin from complete blood flow occlusion exhibited lower damage levels and no FLASH sparing effect. Measures of baseline pO_2 and radiolytic consumption, g_{O2}, during UHDR irradiation confirmed that they were related especially in non-ulcered skin at lower pO_2, and both were significantly related to the likelihood of skin ulceration.

These findings suggest that FLASH sparing which involves oxygen as a primary modulator, where the effect is only present for low levels of oxygen-mediated damage. Anoxic radiation damage

from non-ROS interactions appears to be unaltered by dose rate. The fact that FLASH sparing was also only present when there were lower levels of oxygen suggests that there is a modulating effect from oxygen that should be further investigated to see if it is a causal factor or a correlated biomarker.

References

1. Hall, E.J. and A.J. Giaccia, *Radiobiology for the radiologist*. Eighth edition. ed. 2019, Philadelphia: Wolters Kluwer. vii, 597 pages.
2. Wardman, P., *Chemical radiosensitizers for use in radiotherapy.* Clin Oncol (R Coll Radiol), 2007. **19**(6): p. 397-417.
3. Kirbysmith, J.S. and G.W. Dolphin, *Chromosome Breakage at High Radiation Dose-Rates.* Nature, 1958. **182**(4630): p. 270-271.
4. Dewey, D.L. and J.W. Boag, *Modification of the Oxygen Effect When Bacteria Are Given Large Pulses of Radiation.* Nature, 1959. **183**(4673): p. 1450-1451.
5. Hornsey, S. and D.K. Bewley, *Hypoxia in Mouse Intestine Induced by Electron Irradiation at High Dose-Rates.* International Journal of Radiation Biology and Related Studies in Physics Chemistry and Medicine, 1971. **19**(5): p. 479-&.
6. Petersson, K., G. Adrian, K. Butterworth, and S.J. McMahon, *A Quantitative Analysis of the Role of Oxygen Tension in FLASH Radiation Therapy.* International Journal of Radiation Oncology Biology Physics, 2020. **107**(3): p. 539-547.
7. Tavakkoli, A.D., M.A. Clark, A. Kheirollah, A.M. Sloop, H.E. Soderholm, N.J. Daniel, A.F. Petusseau, Y.H. Huang, C.R. Thomas, Jr., L.A. Jarvis, R. Zhang, B.W. Pogue, D.J. Gladstone, and P.J. Hoopes, *Anesthetic Oxygen Use and Sex Are Critical Factors in the FLASH Sparing Effect.* Adv Radiat Oncol, 2024. **9**(6): p. 101492.
8. Favaudon, V., L. Caplier, V. Monceau, F. Pouzoulet, M. Sayarath, C. Fouillade, M.F. Poupon, I. Brito, P. Hupe, J. Bourhis, J. Hall, J.J. Fontaine, and M.C. Vozenin, *Ultrahigh dose-rate FLASH irradiation increases the differential response between normal and tumor tissue in mice.* Sci Transl Med, 2014. **6**(245): p. 245ra93.
9. Vaupel, P., A.B. Flood, and H.M. Swartz, *Oxygenation Status of Malignant Tumors vs. Normal Tissues: Critical Evaluation and Updated Data Source Based on Direct Measurements with pO2 Microsensors.* Applied Magnetic Resonance, 2021. **52**(10): p. 1451-1479.
10. Hall, E.I. and I.G. Amato, *Radiobiology for the Radiologist*. 8th ed. 2018: Wolters Kluwer.
11. Grimes, D.R. and M. Partridge, *A mechanistic investigation of the oxygen fixation hypothesis and oxygen enhancement ratio.* Biomed Phys Eng Express, 2015. **1**(4): p. 045209.
12. Cao, X., R. Zhang, T.V. Esipova, S.R. Allu, R. Ashraf, M. Rahman, J.R. Gunn, P. Bruza, D.J. Gladstone, B.B. Williams, H.M. Swartz, P.J. Hoopes, S.A. Vinogradov, and B.W. Pogue, *Quantification of Oxygen Depletion During FLASH Irradiation In Vitro and In Vivo.* Int J Radiat Oncol Biol Phys, 2021. **111**(1): p. 240-248.
13. El Khatib, M., A.O. Motlagh, J.N. Beyer, T. Troxler, S.R. Allu, Q. Sun, G.M. Burslem, and S.A. Vinogradov, *Direct Measurements of FLASH-Induced Changes in Intracellular Oxygenation.* International Journal of Radiation Oncology Biology Physics, 2024. **118**(3): p. 781-789.
14. Grilj, V., R.J. Leavitt, M. El Khatib, R. Paisley, J. Franco-Perez, B. Petit, P. Ballesteros-Zebadua, and M.C. Vozenin, *In vivo measurements of change in tissue oxygen level during irradiation reveal novel dose rate dependence.* Radiotherapy and Oncology, 2024. **201**.
15. Sunnerberg, J.P., A.D. Tavakkoli, A.F. Petusseau, N.J. Daniel, A.M. Sloop, W.A. Schreiber, J. Gui, R. Zhang, H.M. Swartz, P.J. Hoopes, D.J. Gladstone, S.A. Vinogradov, and B.W. Pogue, *Oxygen Consumption In Vivo by Ultra-High Dose Rate Electron Irradiation*

Depends Upon Baseline Tissue Oxygenation. Int J Radiat Oncol Biol Phys, 2025. **121**(4): p. 1053-1062.

16. Jansen, J., J. Knoll, E. Beyreuther, J. Pawelke, R. Skuza, R. Hanley, S. Brons, F. Pagliari, and J. Seco, *Does FLASH deplete oxygen? Experimental evaluation for photons, protons, and carbon ions.* Medical Physics, 2021. **48**(7): p. 3982-3990.
17. El Khatib, M., A.L. Van Slyke, A. Velalopoulou, M.M. Kim, K. Shoniyozov, S.R. Allu, E.E. Diffenderfer, T.M. Busch, R.D. Wiersma, C.J. Koch, and S.A. Vinogradov, *Ultrafast Tracking of Oxygen Dynamics During Proton FLASH.* Int J Radiat Oncol Biol Phys, 2022. **113**(3): p. 624-634.
18. Van Slyke, A.L., M. El Khatib, A. Velalopoulou, E. Diffenderfer, K. Shoniyozov, M.M. Kim, I.V. Karagounis, T.M. Busch, S.A. Vinogradov, C.J. Koch, and R.D. Wiersma, *Oxygen Monitoring in Model Solutions and In Vivo in Mice During Proton Irradiation at Conventional and FLASH Dose Rates.* Radiat Res, 2022. **198**(2): p. 181-189.
19. Sunnerberg, J.P., R. Zhang, D.J. Gladstone, H.M. Swartz, J. Gui, and B.W. Pogue, *Mean dose rate in ultra-high dose rate electron irradiation is a significant predictor for O(2)consumption and H(2)O(2)yield.* Phys Med Biol, 2023. **68**(16).
20. Grilj, V., R.J. Leavitt, M. El Khatib, R. Paisley, J. Franco-Perez, B. Petit, P. Ballesteros-Zebadua, and M.C. Vozenin, *In vivo measurements of change in tissue oxygen level during irradiation reveal novel dose rate dependence.* Radiother Oncol, 2024. **201**: p. 110539.
21. Ha, B., K. Liang, C. Liu, S. Melemenidis, R. Manjappa, V. Viswanathan, N. Das, R. Ashraf, B. Lau, L. Soto, E.E. Graves, J. Rao, B. Loo, and G. Pratx, *Real-time optical oximetry during FLASH radiotherapy using a phosphorescent nanoprobe.* Radiotherapy and Oncology, 2022. **176**: p. 239-243.
22. Jansen, J., E. Beyreuther, D. García-Calderón, L. Karsch, J. Knoll, J. Pawelke, M. Schürer, and J. Seco, *Changes in Radical Levels as a Cause for the FLASH effect: Impact of beam structure parameters at ultra-high dose rates on oxygen depletion in water.* Radiotherapy and Oncology, 2022. **175**: p. 193-196.
23. Cao, X., R.X. Zhang, T.V. Esipova, S.R. Allu, R. Ashraf, M. Rahman, J.R. Gunn, P. Bruza, D.J. Gladstone, B.B. Williams, H.M. Swartz, P.J. Hoopes, S.A. Vinogradov, and B.W. Pogue, *Quantification of Oxygen Depletion During FLASH Irradiation In Vitro and In Vivo.* International Journal of Radiation Oncology Biology Physics, 2021. **111**(1): p. 240-248.
24. National Research Council (U.S.). Committee on the Biological Effects of Ionizing Radiations., *Health effects of exposure to low levels of ionizing radiation : BEIR V*. Beir. 1990, Washington, D.C.: National Academy Press. xiii, 421 p.
25. Duval, K.E.A., E. Aulwes, R. Zhang, M. Rahman, M.R. Ashraf, A. Sloop, J. Sunnerberg, B.B. Williams, X. Cao, P. Bruza, A. Kheirollah, A. Tavakkoli, L.A. Jarvis, P.E. Schaner, H.M. Swartz, D.J. Gladstone, B.W. Pogue, and P.J. Hoopes, *Comparison of Tumor Control and Skin Damage in a Mouse Model after Ultra-High Dose Rate Irradiation and Conventional Irradiation.* Radiat Res, 2023. **200**(3): p. 223-231.
26. Rahman, M., J. Kozelka, J. Hildreth, A. Schonfeld, A.M. Sloop, M.R. Ashraf, P. Bruza, D.J. Gladstone, B.W. Pogue, W.E. Simon, and R. Zhang, *Characterization of a diode dosimeter for UHDR FLASH radiotherapy.* Med Phys, 2023. **50**(9): p. 5875-5883.
27. Tessonnier, T., G. Verona-Rinati, L. Rank, R. Kranzer, A. Mairani, and M. Marinelli, *Diamond detectors for dose and instantaneous dose-rate measurements for ultra-high dose-rate scanned helium ion beams.* Medical Physics, 2024. **51**(2): p. 1450-1459.

28. Singers Sorensen, B., M. Krzysztof Sitarz, C. Ankjaergaard, J. Johansen, C.E. Andersen, E. Kanouta, C. Overgaard, C. Grau, and P. Poulsen, *In vivo validation and tissue sparing factor for acute damage of pencil beam scanning proton FLASH.* Radiother Oncol, 2022. **167**: p. 109-115.
29. Duval, K.E.A., E. Aulwes, R.X. Zhang, M. Rahman, M.R. Ashraf, A. Sloop, J. Sunnerberg, B.B. Williams, X. Cao, P. Bruza, A. Kheirollah, A. Tavakkoli, L.A. Jarvis, P.E. Schaner, H.M. Swartz, D.J. Gladstone, B.W. Pogue, and P.J. Hoopes, *Comparison of Tumor Control and Skin Damage in a Mouse Model after Ultra-High Dose Rate Irradiation and Conventional Irradiation.* Radiation Research, 2023. **200**(3): p. 223-231.
30. Pogue, B.W., W.S. Thomas, A.D. Tavakkoli, L.A. Jarvis, and P.J. Hoopes, *Major contributors to FLASH sparing efficacy emerge from murine skin studies: dose rate, total dose per fraction, anesthesia and oxygenation.* Front Oncol, 2024. **14**: p. 1414584.
31. Noda, S., M. Iwakawa, T. Ohta, M. Iwata, M. Yang, M. Goto, H. Tanaka, Y. Harada, and T. Imai, *Inter-strain variance in late phase of erythematous reaction or leg contracture after local irradiation among three strains of mice.* Cancer Detect Prev, 2005. **29**(4): p. 376-82.
32. Esipova, T.V., A. Karagodov, J. Miller, D.F. Wilson, T.M. Busch, and S.A. Vinogradov, *Two new "protected" oxyphors for biological oximetry: properties and application in tumor imaging.* Anal Chem, 2011. **83**(22): p. 8756-65.
33. Cooper, C.R., D. Jones, G.D. Jones, and K. Petersson, *FLASH irradiation induces lower levels of DNA damage ex vivo, an effect modulated by oxygen tension, dose, and dose rate.* Br J Radiol, 2022. **95**(1133): p. 20211150.
34. Leavitt, R.J., A. Almeida, V. Grilj, P. Montay-Gruel, C. Godfroid, B. Petit, C. Bailat, C.L. Limoli, and M.C. Vozenin, *Acute Hypoxia Does Not Alter Tumor Sensitivity to FLASH Radiation Therapy.* Int J Radiat Oncol Biol Phys, 2024. **119**(5): p. 1493-1505.
35. Iturri, L., A. Bertho, C. Lamirault, E. Brisebard, M. Juchaux, C. Gilbert, J. Espenon, C. Sebrie, L. Jourdain, L. de Marzi, F. Pouzoulet, J. Muret, P. Verrelle, and Y. Prezado, *Oxygen supplementation in anesthesia can block FLASH effect and anti-tumor immunity in conventional proton therapy.* Commun Med (Lond), 2023. **3**(1): p. 183.
36. Montay-Gruel, P., M.M. Acharya, K. Petersson, L. Alikhani, C. Yakkala, B.D. Allen, J. Ollivier, B. Petit, P.G. Jorge, A.R. Syage, T.A. Nguyen, A.D. Baddour, C. Lu, P. Singh, R. Moeckli, F. Bochud, J.F. Germond, P. Froidevaux, C. Bailat, J. Bourhis, M.C. Vozenin, and C.L. Limoli, *Long-term neurocognitive benefits of FLASH radiotherapy driven by reduced reactive oxygen species.* Proceedings of the National Academy of Sciences of the United States of America, 2019. **116**(22): p. 10943-10951.
37. Adrian, G., E. Konradsson, M. Lempart, S. Bäck, C. Ceberg, and K. Petersson, *The FLASH effect depends on oxygen concentration.* British Journal of Radiology, 2020. **93**(1106).
38. Favaudon, V., R. Labarbe, and C.L. Limoli, *Model studies of the role of oxygen in the FLASH effect.* Med Phys, 2022. **49**(3): p. 2068-2081.